Structure and decay of a three-quasiparticle isomer in ^{153}Eu

J. F. Smith, S. J. Dorning, B. J. Varley, and W. R. Phillips
Schuster Laboratory, University of Manchester, Manchester M13 9PL, United Kingdom

Ch-. Vieu, J. S. Dionisio, and C. Schuck
Centre de Spectrometrie Nucléaire et de Spectrometrie de Masse, F-91405 Orsay, France

M. Pautrat
Institut de Physique Nucléaire, BP no. 1, F-91406 Orsay, France

(Received 28 February 2000; published 21 August 2000)

An isomer has been observed in the stable nuclide ^{153}Eu, which primarily decays via a 919-keV gamma ray to the $17/2^{+}$ level of the ground-state band. The structure of the isomer has been investigated using an array of eight germanium detectors and an electron spectrometer. The *K*-shell internal-conversion coefficient of the 919-keV transition has been measured to be $9.8(2.4)\times10^{-4}$ establishing that this transition has electric-dipole character. This measurement, and the observed decays of the isomer, indicate that the isomer has spin and parity $19/2^{-}$. Using timing measurements against a pulsed beam, the half-life of the isomer has been measured to be 475(10) ns: this suggests high purity for the *K* quantum number and associated highly *K*-forbidden decays. The gamma-gamma coincidence data have revealed a rotational band built upon the isomer. The properties of the rotational band are consistent with the configurations $\nu[651]3/2\otimes\nu[505]11/2\otimes\pi[413]5/2$, and $\nu[402]3/2\otimes\nu[505]11/2\otimes\pi[413]5/2$, or a mixture of both.

PACS number(s): 21.10.Re, 21.60.Ev, 23.20.Lv, 27.70.+q

I. INTRODUCTION

In deformed, axially-symmetric nuclei, the component of angular momentum along the deformation axis, $K\hbar$, is a constant of the motion. If the *K* quantum numbers of states involved in gamma-ray transitions are good, but differ significantly, the decays are said to be ''*K*-forbidden'' and the decay rates are retarded. For a multi-quasiparticle state, the *K* quantum number is equal to a combination of the *K* values of the individual quasiparticles. If the individual *K* values combine to give a high resultant value, the *K* quantum number of the resulting level, and of levels in the rotational band based upon it, may differ considerably from those of levels based on single quasiparticle states close to the ground state. Transitions between levels based on a multi-quasiparticle state and levels based on single quasiparticle states are then several times *K*-forbidden. In this manner, isomers may arise [1] with long lifetimes, sometimes exceeding several hours: there is now a large amount of experimental information about isomers in the rare-earth region [2–8]. The degree of retardation of the transitions can give information about the purity of the *K* quantum numbers involved in the decays, and properties of rotational bands based on isomers can reveal their intrinsic structure. Recently, attention has been focused on the strong variation in the extent to which transitions are *K* forbidden. The reasons for the variation are not clear: it has been hypothesized to be related to departures from axially symmetric deformation, with the consequence that *K* is no longer a good quantum number [9], and also to mixing with nearby states of different *K* value, but with similar spin and parity [10].

The nucleus ^{153}Eu has been extensively studied [11–15], and bands based on intrinsic configurations with $K^{\pi}=5/2^{+}$, $5/2^{-}$ and $3/2^{+}$ are now known to high spin. Furthermore, a recent publication [16] has reported the existence of an isomer with a half-life of ~8 ns at an excitation energy of 3100 keV, and with spin quantum number near 35/2. The present work was motivated by an earlier study [17] in which tentative evidence for an isomer was observed, with a lifetime estimated to between 400 and 500 ns. In the present work, an isomer has been observed in ^{153}Eu at an excitation energy of 1772 keV, and its properties have been investigated using gamma-ray and electron spectroscopy. The spin and parity of the isomer have been determined to be $19/2^{-}$ from its decay modes, and from a measurement of the internal-conversion coefficient of the most intense decay transition. The magnetic moment of the isomer has been estimated from gamma-ray branching ratios from rotational states built on the isomer. The observed properties of the isomer and its decays are consistent with two possible three-quasiparticle configurations. The present work also extends the bands reported in earlier work: the gamma-gamma coincidence data reveal a change of structure in the lowest negative-parity band at an excitation energy near 3100 keV, but are unable to confirm the scheme proposed in Ref. [16].

II. EXPERIMENTAL DETAILS

Excited states in ^{153}Eu were populated using the ^{150}Nd(^{7}Li,4*n*) reaction. Gamma rays and electrons were observed using an array of eight, 75%-efficient, Eurogam-type [18] germanium detectors and an electron spectrometer. A schematic representation of the apparatus used is shown in Fig. 1. The ^{7}Li beam at energy 35 MeV was provided by the tandem accelerator of the IPN laboratory, Orsay. The beam was pulsed with a pulse width of 2 ns, and was used to bombard thin ^{150}Nd targets, with thicknesses of 200 and 300 μg cm^{-2}. The targets were prepared in the electromag-

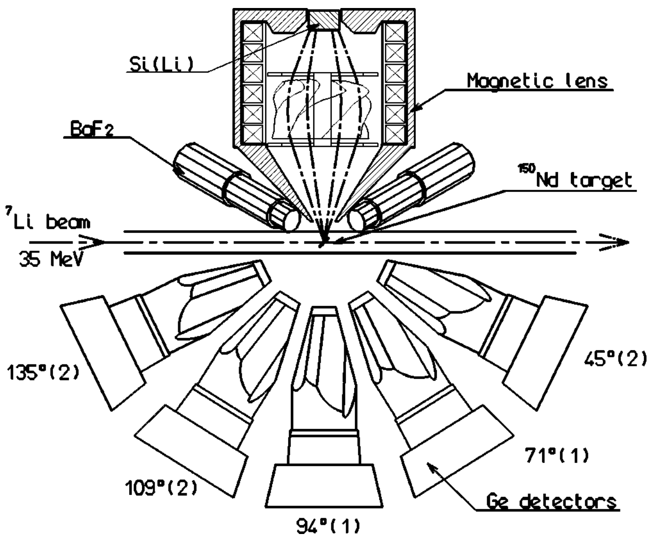

FIG. 1. Schematic representation of the apparatus, as seen from above. Only two of the six BaF_2 detectors are shown. The values written close to the germanium (Ge) detectors give the polar angle, θ, and the number of detectors (in parentheses) at that value of θ.

netic separator at the CSNSM laboratory, Orsay by collecting separated ^{150}Nd ions onto 40-μg/cm^2 carbon backings. The isotopic enrichment of the targets was $>98\%$ and the dominant evaporation residue resulting from the reaction was ^{153}Eu.

The electron spectrometer has been described in detail in Refs. [19,20]. In essence, the spectrometer has a transmission of 4% and a momentum window of 30%, and uses a Si(Li) detector to detect electrons. In the present experiment, it was positioned at 90° to the incident beam. The magnetic field was either swept, or set at fixed values in order to measure internal-conversion coefficients of medium- or high-energy transitions, with the full transmission. The targets were inclined at 30° or 45° to the beam with the carbon backing downstream and facing the electron spectrometer. The germanium detectors were placed approximately azimuthally opposite the electron spectrometer, with the detectors at polar angles between 45° and 135° to the beam direction, as shown in Fig. 1. An array of six barium fluoride (BaF_2) detectors was placed close to the target. The BaF_2 array detected both neutrons and gamma rays emitted from the reaction site, and the fast outputs provided a time reference for the individual germanium and Si(Li) detectors. The number of BaF_2 detectors firing was recorded, and subsequently used as a multiplicity filter. When $\geqslant 1$ signal was detected in the BaF_2 array, and $\geqslant 2$ germanium detectors fired, the energies and times of the gamma rays detected in the germanium detectors were recorded on magnetic ''Exabyte'' tape, together with several other associated parameters such as germanium-detector identification number: a total of approximately 50×10^6 events were collected. Each event occupied approximately 54 bytes, resulting in a total of about 3 Gb of data. In addition to the coincidence data on tape, ''singles'' germanium and Si(Li) detector spectra were incremented for each detector, irrespective of the BaF_2 array.

The experiment consisted of two parts. In the first part the beam was pulsed with a period of $\Delta t = 200$ ns. From these data, ''out-of-beam,'' delayed gamma-ray and electron spectra were incremented, from which the internal-conversion coefficients of transitions de-exciting isomers could be measured. In the second part of the experiment, the beam was pulsed with $\Delta t = 800$ ns in order to measure the lifetime of the isomer, which was expected to be between 400 and 500 ns.

III. ANALYSIS AND RESULTS

A. The level scheme associated with the isomer

A two-dimensional spectrum, or ''matrix,'' containing all the gamma-gamma coincidence events (with no time condition) was constructed, which contained 55×10^6 counts. Gating on known gamma rays confirmed the level scheme for ^{153}Eu presented in earlier work [13–15]. A second matrix containing only those gamma-gamma coincidence events which occurred between 25 and 145 ns after beam pulses, was also constructed and revealed the existence of an isomer in ^{153}Eu at an excitation energy of 1772 keV, decaying pri-

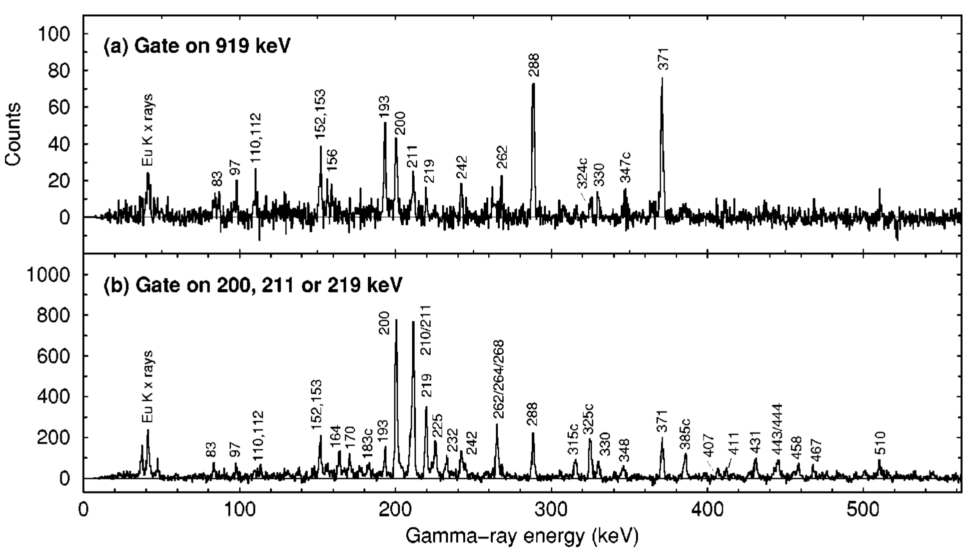

FIG. 2. Spectra of coincident gamma rays in ^{153}Eu. The labels close to the peaks give gamma-ray energies in keV. All labeled peaks correspond to gamma rays in ^{153}Eu apart from those marked with ''*c*,'' which are contaminants from neighboring nuclei.

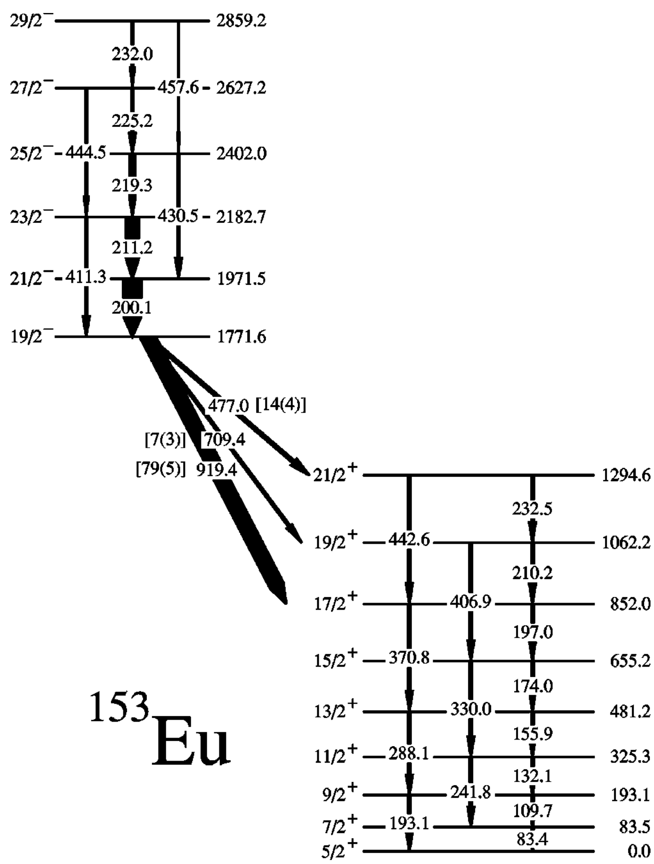

FIG. 3. Partial decay scheme of levels in the band based on the isomer at 1772 keV, and decays of the isomer to the ground-state band. The numbers to the right of the levels, and those centered on the arrows give the level and gamma-ray energies, respectively; the values are in keV and are typically accurate to 0.4 keV. The numbers in square parentheses give relative intensities of gamma rays de-exciting the isomer. The complete known level scheme is given in Ref. [13].

marily via a 919-keV gamma ray. Figure 2(a) shows part of the spectrum of gamma rays in coincidence with the 919-keV transition, obtained from the matrix containing all coincident events (no time gate). Transitions within the ground-state band, following the decay of the isomer (such as 193, 288, and 371 keV) can clearly be seen. In addition, several other transitions (such as 200, 211, and 219 keV) are in coincidence with the 919-keV transition; these transitions are not already known in the level scheme of ^{153}Eu. Figure 2(b) shows the sum of spectra gated on either the 200-, 211-, or 219-keV gamma rays. By applying such gates on these ''new'' transitions, and using energy- and intensity-balance arguments, a rotational band was deduced, built upon the isomer. The levels above the isomer, and those to which the isomer decays are shown in Fig. 3. The isomer, and the levels above it, were only very weakly populated, and as a result it was not possible to use any type of angular-distribution or angular-correlation measurement, to determine the multipolarities of transitions in the band above the isomer, or those decaying from the isomer itself. However, in the band, the characteristic pattern of $\Delta I=1$ transitions and $\Delta I=2$ crossover transitions strongly supports the $E2$ and $M1/E2$ assignments shown on Fig. 3.

B. Internal-conversion coefficient measurement

The most intense transition in the decay of the isomer is a gamma ray of energy 919 keV, which goes to the $17/2^+$ member of the ground-state band. There are also two less intense gamma-ray transitions from the isomer, with energies 709 keV and 477 keV, decaying to the $19/2^+$ and $21/2^+$ members of the ground-state band, respectively. The branching ratios of transitions de-populating the isomer are shown on Fig. 3 as numbers in square parentheses alongside the energies of the gamma rays. The non-observation of other gamma rays decaying from the isomer to other members of the ground-state band, or to members of the $K^\pi=5/2^-$ or $K^\pi=3/2^+$ bands [13] means that their intensities must be less than 3% of the intensity of the 919-keV gamma ray. If it is assumed that electric octupole ($E3$) and magnetic quadrupole ($M2$) transitions do not compete in this situation with electric ($E1$) and magnetic ($M1$) dipole, and electric quadrupole ($E2$) transitions, then these observations restrict the spin and parity of the isomer to be $17/2^+$, $19/2^+$, $21/2^+$, or $19/2^-$.

The spin and parity of the isomer have been investigated by measuring the internal-conversion coefficient of the 919-keV transition. The electron from K-shell internal conversion of the 919-keV transition has an energy of 870 keV, equal to 919 keV less the 49-keV binding energy of a K electron in europium. The K-shell internal-conversion coefficient for the 919-keV transition was determined by comparing the intensity of the 919-keV gamma ray, to that of the 870-keV electron. Normalizations were made, using the similar comparison for the known $E2$ 288- and 371-keV transitions, which have known internal-conversion coefficients. The conversion-coefficient is then given by

$$\alpha_K(919)=k\frac{N_{eK}(870)}{N_\gamma(919)}, \tag{1}$$

where N_γ and N_{eK} are the numbers of gamma rays and electrons, after correction for the relative efficiencies of the detectors as a function of energy, and where k is the normalization factor extracted from the measurements with the 288- and 371-keV $E2$ transitions.

Figure 4(a) shows delayed electrons over an energy range centered on the energy of K-shell internal conversion for the 919-keV transition. The electrons were observed in the interval from 40 to 160 ns after a beam burst. Figures 4(b) and 4(c) show electrons observed over energy ranges centered on 322 keV and 239 keV, respectively: these are the energies of the K-conversion electrons from the 371-keV $17/2^+\rightarrow 13/2^+$ and 288-keV $13/2^+\rightarrow 9/2^-$ transitions in europium, respectively. Figure 5 shows part of the spectrum of gamma rays observed in one of the germanium detectors during the time period from 25 to 145 ns after a beam pulse. In that spectrum there are several peaks with significant intensities close to the 919-keV transition; in order to fully understand the spectrum, these transitions should be explained. The gamma rays at 897 and 1014 keV arise from inelastic scattering of neutrons off bismuth (in the BGO Compton suppression shields) and aluminum (in the target frame, target

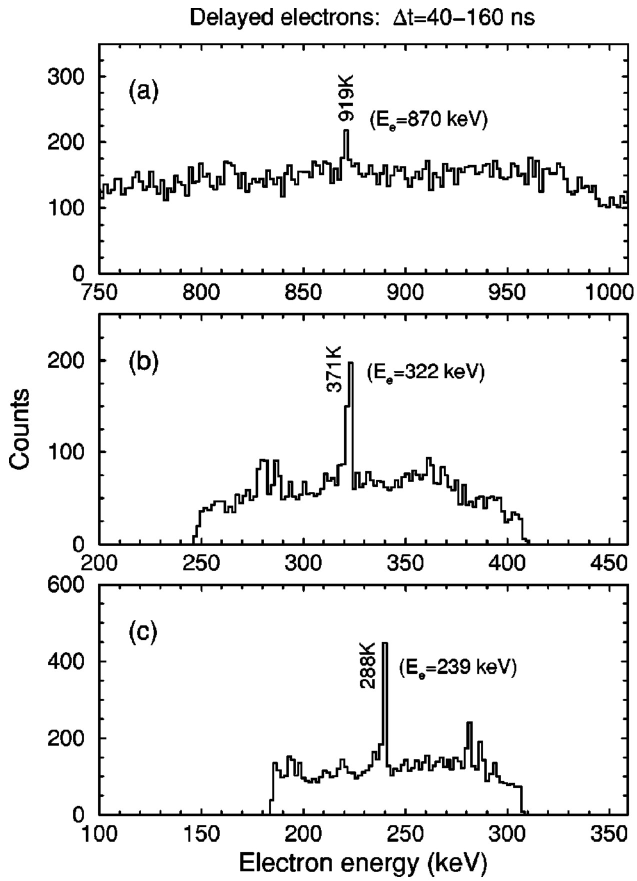

FIG. 4. Delayed *K*-shell internal-conversion electrons of the (a) 919-keV, (b) 371-keV, and (c) 288-keV transitions, observed 40 to 160 ns after beam pulses. The energies of the *K*-conversion lines of interest are shown in keV.

chamber, and detector canisters). The broad peaks between 550 and 850 keV arise from neutron interactions in the neutron detectors. Gating on the 937-keV peak in the gamma-gamma matrix suggests that this transition de-populates a previously unreported isomer in the neighboring $^{154}_{62}$Sm nucleus. The half-life of this isomer has been estimated (from time-gated spectra) to be about 25 ns. This transition is interesting, in that, although the 937-keV gamma-ray peak in Fig. 5 is clearly of comparable intensity to the 919-keV gamma-ray peak, there does not appear to be a samarium K conversion electron peak at 890 keV (that is, 937 keV minus 47-keV binding energy) in Fig. 4(a) corresponding to the 937-keV peak of Fig. 5. The reason for this becomes apparent if it is remembered that the time gate for the delayed electron spectrum of Fig. 4 (40 to 160 ns after a beam pulse) starts later than that for the delayed gamma-ray spectra (25 to 145 ns). Therefore, when the time gate for the electron spectrum starts, the ^{154}Sm isomer has almost passed through two half-lives.

The mean value of $\alpha_K(919)$ determined from the comparisons, with the 288- and 371-keV transitions, is $9.8(2.4)\times10^{-4}$. The theoretical values are 4.6×10^{-3} for an $M1$ transition, 2.7×10^{-3} for an $E2$ transition, and 1.1×10^{-3} for an $E1$ transition. This measurement, together with the observation of the 477- and 709-keV transitions (Fig. 3), therefore establishes that the transition has $E1$ character, that parity of the isomer is negative, and that the spin is probably 19/2.

C. Lifetime measurement

The lifetime of the isomer has been determined by measuring the times at which gamma rays were detected with respect to the beam pulse. This was achieved by constructing a matrix with gamma-ray energy on one axis, and gamma-ray time on the other axis. By gating on a transition on the energy axis, the time spectrum associated with that transition was projected onto the other axis. The lifetime of the isomer was determined in this manner, by gating on the 919-keV transition, and also on the 288- and 371-keV transitions, all of which occur in coincidence following the decay of the isomer. The time spectra of the 919-, 371-, and 288-keV transitions are shown in Figs. 6(a), 6(b), and 6(c), respectively: fits to these time spectra, in the regions clear of the tail of the prompt peaks, gave values of 464(16), 478(17), and 486(18) ns for the half-life, respectively. Taking a weighted mean of these values results in a half-life of 475(10) ns.

IV. DISCUSSION

A. Configuration of the isomer

The structure of ^{153}Eu, up to spins of at least $15\hbar$, can be described [13,21] in terms of rotations of an axially-symmetric, reflection-symmetric, prolate shape with a dominant quadrupole deformation. For quadrupole deformations commonly met in the rare-earth nuclei near $N=90$, $Z=60$ there are several Nilsson orbitals close to the Fermi surface [22–24]. In ^{153}Eu the ground state is associated predominantly with the $\pi[413]5/2^+$ orbital, and the first and

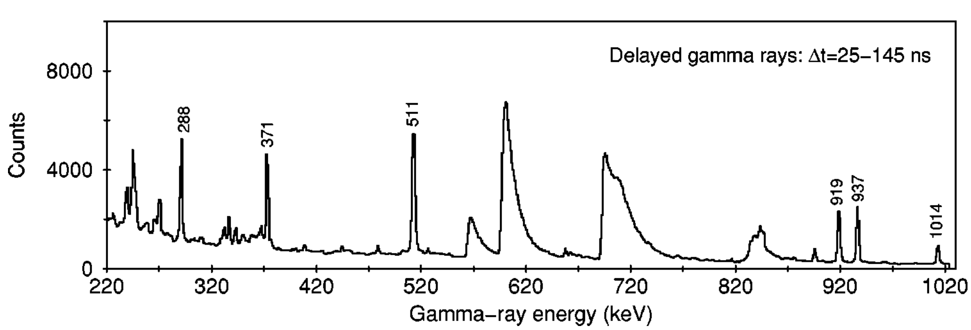

FIG. 5. Delayed gamma rays observed in the time interval 25 to 145 ns after the beam pulses. Some of the peaks are labeled with gamma-ray energies in keV. The labeled peaks are discussed in the text.

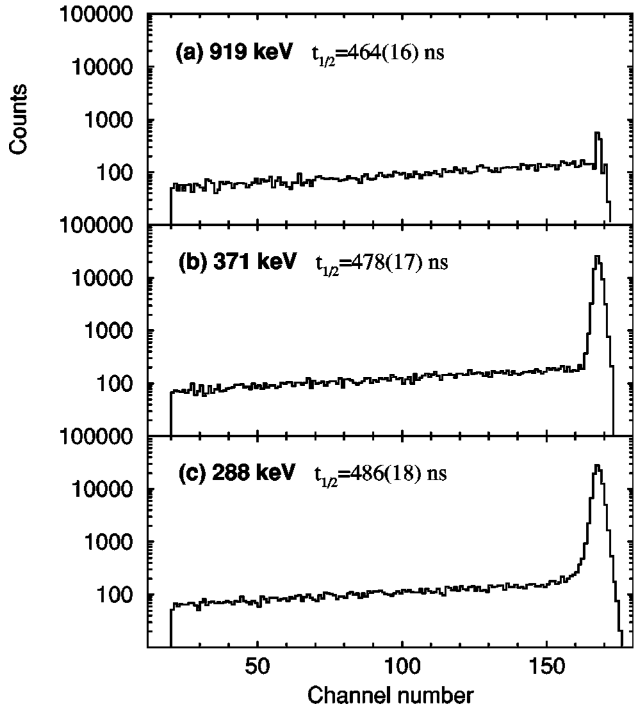

FIG. 6. The time spectra of the (a) 919-keV, (b) 371-keV, and (c) 288-keV transitions. One channel corresponds to 5 ns. The lifetimes deduced by a fit to the spectra are indicated on the panels.

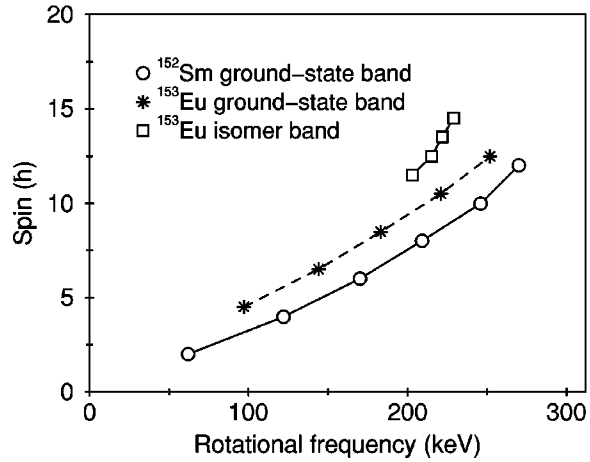

FIG. 7. Spin plotted against rotational frequency for bands in ^{152}Sm and ^{153}Eu.

second intrinsic excited states with the $\pi[532]5/2^-$ and $\pi[411]3/2^+$ orbitals, respectively. With standard parameters [22] used to predict single-particle levels in a deformed well, these assignments are consistent with a quadrupole deformation of $\beta_2 \sim 0.25$–0.30. At this deformation, only proton orbitals with Ω quantum numbers from 1/2 to 7/2, and neutron orbitals with Ω quantum numbers of 1/2, 3/2, 5/2, and 11/2 lie within about 1 MeV of the Fermi surface. Three protons in available orbitals cannot combine to give a state of spin 19/2. In this region, the $\nu[505]11/2$ orbital plays an important role in generating multi-quasiparticle isomers. If a pair of neutrons is broken, resulting in the occupation of an $11/2^-$ orbital, then a high-*K* state can be formed at relatively low excitation energy, where no other states exist with comparable *K* values. In particular, a neutron in a [505]11/2 orbital, and one in a [402]3/2 or [651]3/2 orbital can combine their angular momenta and parities with the [413]5/2 proton to give a state of spin and parity $19/2^-$. These configurations are therefore, prime candidates for the isomer identified in this work.

In the neighboring $^{154,156}_{64}$Gd and $^{152}_{62}$Sm nuclei, isomers of spin and parity 7^- have been previously reported [3,25,26], at excitation energies close to 2100 keV. It has been proposed that they arise by the breaking of a [402]3/2 or [651]3/2 neutron pair, with one of the neutrons promoted to the $[505]11/2^-$ orbital. Comparison with these nuclei suggests that in ^{153}Eu, the most likely configurations of the isomer are $\nu[402]3/2 \otimes \nu[505]11/2 \otimes \pi[413]5/2$ or $\nu[651]3/2 \otimes \nu[505]11/2 \otimes \pi[413]5/2$. An argument against the [651]3/2 neutron orbital playing a major role is provided by the Gallagher-Moszkowski (GM) [27] splittings arising from the residual *p-n* interactions [28,29] when a $\pi[413]5/2^+$ proton is coupled to the separate, assumed pure, two-quasineutron 7^- states. The GM splitting due to the proton interaction with the [651]3/2 neutron (of the $K=19/2$ state) shifts the energy up, while that from the interaction with the [402]3/2 neutron shifts it down. However, this may be counteracted by the unknown relative spacings of the [651]3/2 and [402]3/2 states; it is possible that the [651]3/2 orbital may lie lower than the [402]3/2 orbital.

The alignment in the band based on the isomer can give further information about the isomer configuration. Figure 7 shows the angular momenta of levels in the ground-state band of ^{152}Sm and in the ground-state and isomer bands in ^{153}Eu plotted against rotational frequency. The separation of the curves reveals that there is about 3 or 4 $\hbar$ extra alignment in the isomer band which does not rule out the possibility that the isomer configuration includes the [651]3/2 orbital (which has high total angular momentum but a relatively low component along the symmetry axis). However, there is no way of unambiguously distinguishing the dominance of one of the proposed configurations. In any case, it is highly probable that both configurations are significantly mixed in the $19/2^-$ state.

B. Excitation energy of the isomer

The energy of the isomer and the energies of other multi-quasiparticle states in ^{153}Eu are related to the quasiparticle excitation energies, the energy needed to break a pair, the zero-point rotational energy, and the interaction energies of the coupled particles. Phenomenological models [30,31] have been proposed, to estimate the magnitudes of the separate energy contributions. Here, there is insufficient information for these models to be used with any accuracy. However, it is possible to examine the energy sequence of the multiplet of states which arise from the proposed configuration. The different couplings of angular momenta allow states with spins $\Omega_1 \pm \Omega_2 \pm \Omega_3$, that is, states with *K* quantum numbers 19/2, 13/2, 9/2 and 3/2. In particular, if the 13/2 state is predicted to lie lower than the observed 19/2 level it may be near-yrast and thus it may be anticipated that this

TABLE I. Retardation factors for transitions which follow the decay of the isomer. In calculating the retardations, the Weisskopf estimates have been multiplied by 10^4 to account for the usual strong hindrance of $E1$ transitions; this multiplication factor is often used; for example, see Ref. [8].

Transition	E_γ (keV)	Retardation	f_ν
$19/2^- \rightarrow 17/2^+$	919.4(4)	$2.0(1)\times 10^5$	7.6
$19/2^- \rightarrow 19/2^+$	709.4(4)	$1.0(4)\times 10^6$	10.0
$19/2^- \rightarrow 21/2^+$	477.0(4)	$1.5(4)\times 10^5$	7.3

state will be populated in the present experiment. The GM splittings for the three pairs of interactions between the two neutrons and the proton in the $K=13/2$ level, from the $\nu[402]3/2\otimes\nu[505]11/2\otimes\pi[413]5/2$ configuration are all positive, and so the predicted position of the 13/2 level is above that of the 19/2. In the $K=13/2$ level from the $\nu[651]3/2\otimes\nu[505]11/2\otimes\pi[413]5/2$ configuration, two of the GM splittings lower the energy of the 13/2 state and one raises it, and it is not possible to estimate the relative positions of the 13/2 and 19/2 levels. The non-observation of a candidate for the $13/2^-$ band-head therefore gives no clear indication of the dominant component in the isomer.

C. Decay of the isomer

The degree of retardation of a transition de-populating an isomer is often expressed in terms of the ratio of the measured partial gamma-ray half-life $T^{\gamma}_{1/2}$ to the Weisskopf estimate $T^{W}_{1/2}$. The reduced hindrance factor,

$$f_\nu=(T^{\gamma}_{1/2}/T^{W}_{1/2})^{1/\nu}, \tag{2}$$

is useful for global comparisons of retardations. The parameter ν gives the extent to which a transition is K-forbidden, and

$$\nu=\Delta K-\lambda, \tag{3}$$

for a transition of multipolarity λ, with ΔK being the difference in the K quantum numbers of the levels involved in the transition. The isomer at 1772 keV observed here, presumably has K quantum number 19/2; therefore the $E1$ transitions between the isomer and members of the $K=5/2$ ground-state band, have $\Delta K=7$ and $\nu=6$. The reduced hindrance factors, calculated from the lifetime of the isomer and the measured gamma-ray branching ratios, for the three $E1$ transitions (see Fig. 3) which de-populate the 1772-keV isomer, are given in Table I.

The f_ν values are characteristic of transitions between levels which have a degree of K purity, corresponding to only small amounts of K mixing in the isomer and in the levels in the ground-state band. The retardations have roughly similar values, and the slight differences in magnitude, can be explained by small admixtures of states with different K values into the ground-state band. The shape of the isomer is, therefore, like the ground state, expected to be axially symmetric [13]. This is, perhaps, apparent from the regular structure of the rotational band built on the isomer.

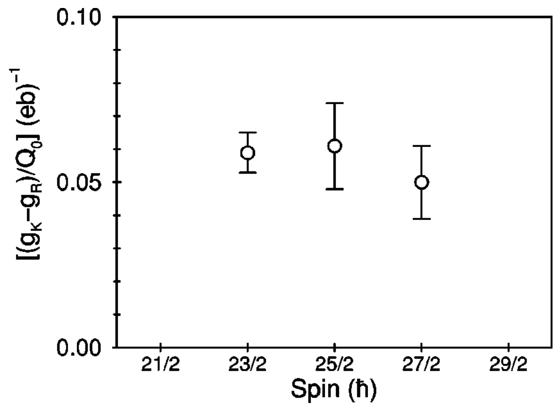

FIG. 8. The magnitudes of $(g_K-g_R)/Q_0$ determined from branching ratios within the isomer band.

D. Rotational band built on the isomer

The axial symmetry and the purity of the K quantum number of the isomer are confirmed by the observation of a regular rotational band with the isomer as band-head. The ratios of the intensities of the $E2$ crossover gamma rays to the mixed $E2/M1$ gamma rays in the band, were used to calculate the ratios $(g_K-g_R)/Q_0$. The ratios are shown in Fig. 8 as a function of spin. The average value determined for the magnitude of $(g_K-g_R)/Q_0$ is 0.058(3) $(e\,\mathrm{b})^{-1}$. Using a value of 6.6(5) e b for the intrinsic quadrupole moment Q_0 as obtained from Coulomb excitation of the ground-state band [15], and a value of 0.40(4) for g_R, values of g_K can be inferred: taking the positive sign for $(g_K-g_R)/Q_0$ gives $g_K=0.78(5)$, while taking the negative-sign gives $g_K=0.02(5)$. The large g_K value (0.78) implies a three-proton configuration for the isomer and so may be disregarded. (The dominant contribution to the uncertainty comes from the assumed uncertainty in the collective g-factor g_R.)

The extracted value of g_K for the isomer can be compared with values predicted for the proposed configurations. For a three-quasiparticle state, in which the individual Ω_i quantum numbers sum maximally, to give the resultant K value,

$$Kg_K=\sum_i \Omega_i g_i, \tag{4}$$

where

$$\Omega_i g_i=g_{i,s}\langle s_z\rangle+g_{i,l}\langle l_z\rangle \tag{5}$$

and

$$K=\sum \Omega_i. \tag{6}$$

The first term on the right-hand side of Eq. (5) gives the contribution from the intrinsic spin, and the second gives that due to orbital nucleon motion. These contributions can be estimated for each quasiparticle, in order to estimate the g_K value for each configuration. The estimated value can then be compared to the value extracted for the isomer. For a neutron in the [505]11/2 orbital, $g_{i,l}$ is zero and the spin is fully aligned along the z-axis. Thus $\Omega_i g_i=g_{i,s}\langle s_z\rangle\approx-1.15$,

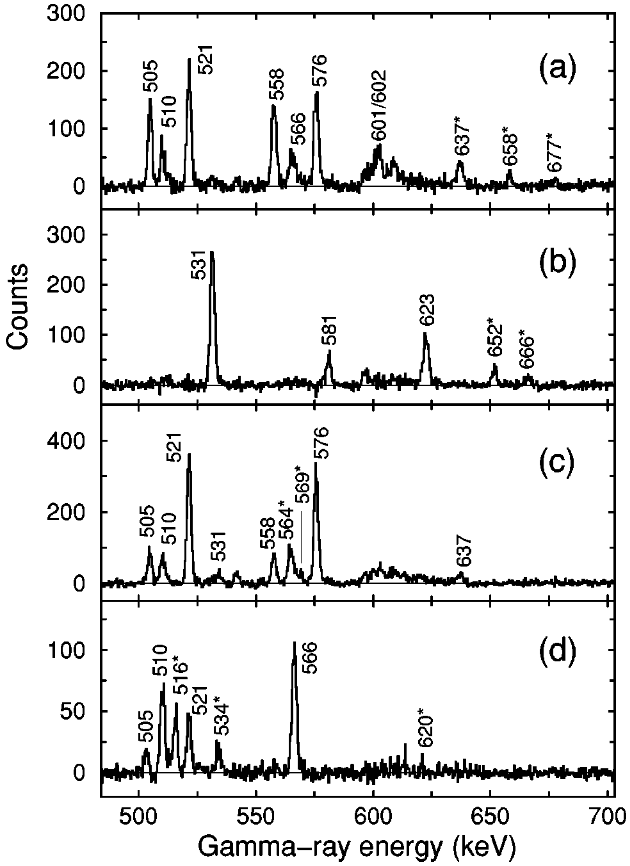

FIG. 9. Representative gamma-gamma coincidence spectra. Panels (a) and (b) show the ground-state band: (a) is the sum of spectra obtained by gating on the 602-, 637-, and 658-keV transitions; and (b) is the sum of spectra obtained by gating on the 581-, 623-, and 659-keV transitions. Panels (c) and (d) show the $K^\pi = 5/2^-$ band: (c) is gated on the 601-keV transition; and (d) is gated on the 593-keV transition. The labels on the spectra give the transition energies to the nearest keV, and all of the labeled peaks correspond to transitions in ^{153}Eu. The transitions marked with an asterisk have first been observed in the present work.

where the spin g-factor for the neutron has been chosen equal to 0.6 times that of the free neutron. For a proton in the [413]5/2 orbital, the value of $\Omega_i g_i$ may be obtained from the measured moment [11] of 1.533(1) μ_N for the ^{153}Eu ground state. The magnetic moment of a state of spin I is given by the formula

$$\mu = I(g_R + I g_K)/(I+1), \tag{7}$$

where μ is expressed in units of nuclear magnetons (μ_N). Substituting a value of $0.40(4)(\simeq Z/A)$ for g_R, into Eq. (7) gives $\Omega_i g_i \approx +1.75$ for the [413]5/2 proton. In view of the error on the extracted value of g_K for the isomer, and the influence of the values of $\Omega_i g_i$ for a neutron in the [402]3/2 or [651]3/2 orbitals on the prediction, the $\Omega_i g_i$ values for each of these two possibilities may be estimated to sufficient accuracy by assuming a value of 0.25 for $\langle s_z \rangle$. This gives $\Omega_i g_i = g_{i,s} \langle s_z \rangle \simeq -0.57$.

The three $\Omega_i g_i$ values can now be combined, using Eq. (4), to give a predicted g_K for the isomer of ~ 0.03 for both

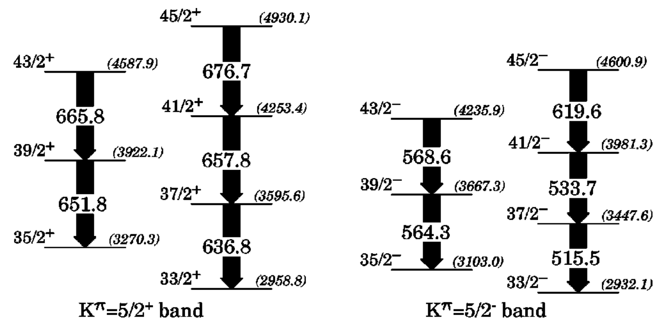

FIG. 10. Partial high-spin level scheme for the $K^\pi = 5/2^+$ and $K^\pi = 5/2^-$ bands. The figure shows the highest spin level reported in Ref. [13], together with the extensions to the bands observed in the present data. The uncertainties on the transition and level energies are about 0.2 keV.

configurations. This value is consistent with that determined from the branching ratios of the levels in the isomer band when the negative sign is taken for $(g_K - g_R)/Q_0$.

E. Band-crossing at high spin

In the work of Ref. [16], it has been reported that the $35/2^-$ level of the $K^\pi = 5/2^-$ band is isomeric, with a lifetime of 8 ns. The lifetime measurement was based on delayed coincidences between a 635-keV gamma ray feeding into the $35/2^-$ level and a 600-keV gamma ray de-exciting the same level. In the present work, the high-spin bands presented in Refs. [13,14] have been extended to still higher spins. Figure 9 shows representative gamma-gamma coincidence spectra, which reveal the ''new'' transitions at the highest spins, and Fig. 10 shows the partial high-spin level scheme for the extended bands. (For the complete level scheme, see Ref. [13].)

Figure 11 shows the $\mathcal{J}^{(1)}$ kinematic moments of inertia of these bands, plotted against rotational frequency. A backbend occurs in the negative-parity band at a frequency ~ 0.25 MeV indicating a change of structure, as was sug-

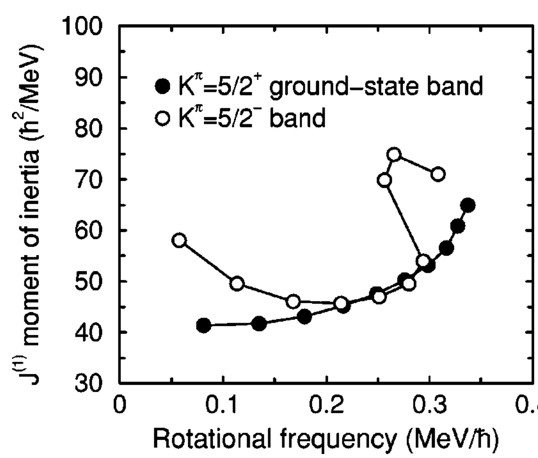

FIG. 11. Kinematic $\mathcal{J}^{(1)}$ moments of inertia plotted against rotational frequency for the $K^\pi = 5/2^+$ ground-state band, and the $K^\pi = 5/2^-$ band in ^{153}Eu. Only one signature partner of each band is shown.

gested in Ref. [16]. The positive-parity band exhibits an upbend, suggesting a strong interaction between the crossing bands while the negative-parity band shows a back-bend, suggestive of a weak interaction. The crossing frequency is characteristic of the alignment of a pair of $i_{13/2}$ neutrons, in this region.

The long lifetime of the $35/2^-$ level reported in Ref. [16] is difficult to understand in view of the extensions to the known bands observed here. It should be pointed out that the deduction of the level properties from gamma-ray spectroscopic information, in the region of excitation energy close to the $35/2^-$ level, is made difficult by the broad distribution of events arising from inelastic scattering to the 596-keV level in ^{74}Ge (of the germanium detectors), by the presence of gamma rays of energy 637 keV and 602 keV in the $K^\pi = 5/2^+$ ground-state band, and by a gamma ray of energy 601 keV in the $K^\pi = 5/2^-$ band. In this work, it was not possible to confirm that a 635-keV gamma ray feeds into the $35/2^-$ level, or that the 635-keV gamma ray is in coincidence with a 690-keV gamma ray, as were both reported in Ref. [16].

V. SUMMARY

In summary, an isomer has been identified in ^{153}Eu, at an excitation energy of 1772 keV. The isomer has been investigated using gamma-ray and electron spectroscopic techniques. An array of eight 75%-efficient Eurogam-type germanium detectors, and an electron spectrometer have been used. The isomer is observed to decay primarily via a 919-keV gamma-ray transition, into the $17/2^-$ state of the ground-state band. The K-shell internal-conversion coefficient of the 919-keV transition has been measured to be $9.8(2.4)\times 10^{-4}$, suggesting that it has $E1$ character. This measurement, together with observed weaker decay paths, suggests that the isomer has spin and parity of $19/2^-$. The lifetime of the isomer has been measured to be 475(10) ns, using a pulsed beam with period of 800 ns. Gamma-gamma coincidence data have revealed a rotational band built on the isomer, consisting of $\Delta I = 2$ $E2$ and $\Delta I = 1$ $M1/E2$ transitions. The spin and parity assignment of the isomer, together with the observed properties of the rotational band, are consistent with two proposed three-quasiparticle configurations, both involving an high-Ω $h_{11/2}$ neutron. Furthermore the previously established high-spin bands have been extended to higher spins and have revealed a band-crossing at rotational frequency $\hbar\omega = 0.28$ MeV/$\hbar$, which is presumed to be due to $i_{13/2}$ neutrons.

ACKNOWLEDGMENTS

The authors would like to thank the accelerator staff, at the IPN tandem laboratory, in Orsay. We would also like to thank the electromagnetic separator group of CSNSM for the fabrication of the targets. The authors are grateful for financial support from the Alliance project, which is funded by the Agence pour l'Accueil des Personnalitès in France, and the British Council.

[1] R. G. Helmer and C. W. Reich, Nucl. Phys. **A114**, 649 (1968).
[2] H. Hübel, R. A. Naumann, and P. K. Hopke, Phys. Rev. C **2**, 1447 (1970).
[3] L. L. Riedinger, D. C. Sousa, E. G. Funk, and J. W. Mihelich, Phys. Rev. C **4**, 1352 (1971).
[4] E. Schoeters, R. E. Silverans, L. Vanneste, K. Freitag, and H. Hübel, Z. Phys. A **272**, 203 (1975).
[5] P. M. Walker, D. M. Cullen, C. S. Purry, D. E. Appelbe, A. P. Byrne, G. D. Dracoulis, T. Kibédi, F. G. Kondev, I. Y. Lee, A. O. Machiavelli, A. T. Reed, P. H. Regan, and F. Xu, Phys. Lett. B **408**, 42 (1997).
[6] A. M. Bruce, A. P. Byrne, G. D. Dracoulis, W. Gelletly, T. Kibédi, F. G. Kondev, C. S. Purry, P. H. Regan, C. Thwaites, and P. M. Walker, Phys. Rev. C **55**, 620 (1997).
[7] K. Jessen, M. Bergstrom, P. von Brentano, A. Dewald, B. Herskind, H. Meise, C. Schumacher, G. Sletten, O. Stuck, D. Weisshaar, I. Wiedenhover, and J. Wrzesinski, Eur. Phys. J. A **2**, 113 (1998).
[8] R. D'Alarco, P. Chowdhury, E. H. Seabury, P. M. Walker, C. Wheldon, I. Ahmad, M. P. Carpenter, G. Hackman, R. V. F. Janssens, T. L. Khoo, C. J. Lister, D. Nisius, P. Reiter, D. Seweryniak, and I. Wiedenhover, Phys. Rev. C **59**, R1227 (1999).
[9] B. Crowell, P. Chowdhury, D. J. Blumenthal, S. J. Freeman, C. J. Lister, M. G. Carpenter, R. G. Henry, R. V. F. Janssens, T. L. Khoo, T. Lauritsen, Y. Liang, F. Soramel, and I. G. Bearden, Phys. Rev. C **53**, 1173 (1996).
[10] F. G. Kondev, M. A. Riley, D. J. Hartley, R. W. Laird, T. B. Brown, M. Lively, K. W. Kemper, J. Pfohl, S. L. Tabor, and R. K. Sheline, Phys. Rev. C **59**, R575 (1999).
[11] M. A. Lee, Nucl. Data Sheets **37**, 487 (1982); **60**, 419 (1990).
[12] G. D. Dracoulis, J. R. Leigh, M. G. Slocombe, and J. O. Newton, J. Phys. G **1**, 853 (1975).
[13] C. J. Pearson, W. R. Phillips, J. L. Durell, B. J. Varley, W. J. Vermeer, W. Urban, and M. J. Khan, Phys. Rev. C **49**, R1239 (1994).
[14] S. Basu, S. Chattopadhyay, J. M. Chattergee, R. K. Chattopadhyay, S. S. Ghugre, G. O. Rodrigues, R. P. Singh, S. Murulitha, and R. K. Bhowmik, Phys. Rev. C **56**, 1756 (1997).
[15] J. F. Smith, M. W. Simon, R. W. Ibbotson, P. A. Butler, A. Aprahamian, A. M. Bruce, D. Cline, M. Devlin, G. D. Jones, P. M. Jones, and C. Y. Wu, Phys. Rev. C **58**, 3171 (1998).
[16] J. M. Chattergee, S. Basu-Roy, S. S. Ghugre, S. Chattopadhyay, R. P. Singh, G. O. Rodrigues, R. K. Chattopadhyay, and R. K. Bhowmik, Eur. Phys. J. A **1**, 55 (1998).
[17] S. J. Dorning, Ph.D. thesis, University of Manchester, 1998.
[18] C. W. Beausang *et al.*, Nucl. Instrum. Methods Phys. Res. A **313**, 37 (1992).
[19] J. S. Dionisio *et al.*, Nucl. Instrum. Methods Phys. Res. A **362**, 122 (1995).
[20] J. S. Dionisio *et al.*, Nucl. Instrum. Methods Phys. Res. A **437**,

282 (1999).
[21] A. V. Afanasjev and I. Ragnarsson, Phys. Rev. C **51**, 1259 (1995).
[22] R. Bengtsson, J. Dudek, W. Nazarewicz, and P. Olanders, Phys. Scr. **39**, 196 (1989).
[23] A. K. Jain, R. K. Sheline, P. C. Sood, and K. Jain, Rev. Mod. Phys. **62**, 395 (1990).
[24] W. Nazarewicz, M. A. Riley, and J. D. Garrett, Nucl. Phys. **A512**, 61 (1990).
[25] J. Konijn, F. W. N. de Boer, A. V. Poelgeest, W. H. A. Hesselink, M. J. A. de Voigt, and H. Verheul, Nucl. Phys. **A352**, 191 (1981).
[26] J. Konijn, J. B. R. Berkhout, W. H. A. Hesselink, J. J. V. Ruijven, P. V. Nes, H. Verheul, F. W. N. de Boer, C. A. Fields, E. Sugarbaker, P. M. Walker, and R. Bijker, Nucl. Phys. **A373**, 397 (1982).
[27] C. J. Gallagher and S. J. Moszkowski, Phys. Rev. **111**, 1282 (1956).
[28] K. Jain, P. M. Walker, and N. Rowley, Phys. Lett. B **322**, 27 (1994).
[29] A. K. Jain, R. K. Sheline, D. M. Headly, P. C. Sood, D. G. Burke, I. Hrivnacova, J. Kvasil, D. Nosek, and R. W. Hoff, Rev. Mod. Phys. **70**, 843 (1998).
[30] K. Jain and A. K. Jain, Phys. Rev. C **45**, 3013 (1992).
[31] N. I. Pyatov and A. S. Chernyshev, Bull. Acad. Sci. USSR, Phys. Ser. **28**, 1073 (1964).